ACADÉMIE
DES SCIENCES
INSTITUT DE FRANCE

Comptes Rendus
Physique

Anaëlle Givaudan, Francesco Picella and Hélène de Maleprade

Roll formation in a bio-active fluid

Volume 27 (2026), p. 7-16

Online since: 19 January 2026

https://doi.org/10.5802/crphys.268

This article is licensed under the
Creative Commons Attribution 4.0 International License.
http://creativecommons.org/licenses/by/4.0/

The Comptes Rendus. Physique *are a member of the Mersenne Center for open scientific publishing*
www.centre-mersenne.org — e-ISSN : 1878-1535

ACADÉMIE DES SCIENCES
INSTITUT DE FRANCE

Comptes Rendus. Physique
2026, Vol. 27, p. 7-16
https://doi.org/10.5802/crphys.268

Research article

Roll formation in a bio-active fluid

Anaëlle Givaudan [a], Francesco Picella [a] and Hélène de Maleprade [a]

[a] Sorbonne Université, CNRS, Institut Jean Le Rond d'Alembert, Paris 75005, France

E-mails: francesco.picella@sorbonne-universite.fr, helene.de_maleprade@sorbonne-universite.fr

Abstract. Collective motion of micro-swimmers leads to the emergence of coherent macroscopic structures. In the case of diluted cultures of micro-organisms, a typical dotted pattern can spontaneously appear within a few minutes, even in the absence of external stimulus, a signature of bioconvection. However, we know little about the resilience of bioconvective plumes facing an environmental alteration. Here, we take advantage of the phototactic behaviour of the green micro-algae *Chlamydomonas reinhardtii* to perturb bioconvection with an asymmetric lightning. Our experiments demonstrate that plumes first disappear, leaving place for a new anisotropic structure at the illuminated wall. We characterise the dynamics of this rising pattern at various scales and propose a mechanism based on the physical properties of the micro-swimmers.

Keywords. Hydrodynamics, instability, micro-swimmer, active matter.

Manuscript received 20 May 2025, revised 26 October 2025, accepted 7 November 2025, online since 19 January 2026.

1. Introduction

Dilute suspensions of swimming micro-organisms are remarkable, as they spontaneously destabilise: an inhomogeneous concentration pattern emerges. Many species are capable of bioconvection, spanning from bacteria [1], green micro-algae like *Chlamydomonas* [2,3] or *Euglena* [4] species, up to the ciliate *Tetrahymena* [5,6]. Typical sizes of these micro-swimmers therefore range over two orders of magnitude, from 1 µm to 500 µm. In his pioneering work of 1911 on *Euglena viridis*, Wager claims that the patterns he observes are "not due to heat, but are in large measure the mechanical result of the action of gravity combined with cohesive forces acting upon organisms heavier than water" [7]. He points essential ingredients for the onset of bioconvection: the fluid is not set into motion by an external forcing, but rather by an endogenous mechanism. Surprisingly, these denser micro-organisms accumulate at the top of a water bath. Motivations to swim upwards vary across micro-organisms: some swim up oxygen or chemical gradients [8], other align along magnetic [9] or gravitational fields. Indeed, *Euglena* and *Tetrahymena* are bottom heavy, so that gravity naturally reorients them to the top [10,11]. *Chlamydomonas* is also bottom heavy, and this has been the widely accepted reorientation mechanism for the past decades [12], yet works by Hosoya *et al.*, and more recently by Kage *et al.*, demonstrate that bottom heaviness is negligible compared to the effect of flagella [13,14]. Indeed, flagella introduce an additional drag on *Chlamydomonas*, large enough to efficiently reorient algae to the top. Then, once swimmers accumulate at the upper surface in a denser layer, this layer destabilises akin to a Rayleigh–Taylor instability and regions of high concentration in swimmers sink [15]. When they hit a bottom surface, the stream of micro-organisms is ejected radially and the flow goes up again.

As the elongated swimmers experience a torque reorienting them towards concentrated regions, this flow is self-sustained [2].

A characteristic wavelength appears as plumes develop in a diluted culture of micro-swimmers. Among many parameters, this wavelength is controlled by cell concentration, the depth of the bath [16,17], red or white illumination [18], the metabolic activity of cells [19], and time [3,20]. Although many experimental and numerical studies focus on bioconvection [21], plumes' inherent dynamic nature — marked by continuous reorganisation, fusion, and splitting — remains only partially captured. In fact, few studies look at several plumes, without reproducing experimental wavelength transitions [22,23]. This stresses that we nowadays do not fully understand the physical ingredients behind plumes' dynamics. Yet, a common way to gain control over this dynamics is to constrain the system. In micro-algal bioconvection, light is a widely used external parameter, taking advantage of the swimmers photosynthetic and phototactic activity [24,25]. Light imposes new favourite swimming directions, and micro-swimmers accumulate in regions finely tuned by the illumination pattern. A related bioconvective dynamics therefore develops [26]. For example, Arieta *et al.* trigger a single plume at a chosen location, with a laser beam shone horizontally onto a vertical Hele-Shaw cell filled with *Chlamydomonas reinhardtii* (CR) [27]. In a similar geometry, yet rotated horizontally, Dervaux *et al.* use a vertical laser beam hitting a horizontal petri dish filled with a dilute culture of CR. They demonstrate the rise of a circular instability, radially ejecting waves of micro-swimmers [28,29]. These recent experiments all start with a homogeneous population of micro-swimmers, and use light as a tool to specifically design bioconvective patterns. Here, we wonder how light interferes with an already developed bioconvective pattern.

We study the resilience of plumes to an asymmetrical lighting field. Using a diluted culture of CR, we highlight for the first time that a blue light shone through a side wall triggers a strong spatially heterogeneous phototactic reaction. First, plumes of bioconvection vanish close to the illuminated wall. Then, CR accumulate near this wall. Consequently, an unexpected concentration pattern appears in this zone. A strongly anisotropic structure develops orthogonal to the wall, with a wavelength typically three times smaller than initial plumes. We finally explain this anisotropic pattern based on the formation of a bioconvective roll at the enlightened wall, which further destabilises due to the hydrodynamic footprint of our micro-swimmers.

The paper is organised as follow. First, we describe our experimental setup. We then present our experimental observations and finally provide a qualitative explanation about the onset of collective structures.

2. Experimental methods

2.1. *Experimental setup*

Macroscopic experimental setup. We study algae dynamics in a cubic box with length $L = 8\,\mathrm{cm}$. Liquid height is adjusted to $h \in [1; 8]\,\mathrm{mm}$ (see Figure 1). The concentration is $c \in [1; 10] \cdot 10^6\,\mathrm{cells/mL}$. Side walls are opaque, made of 3.2 mm-black-ADA plates (polypropylene). The bottom of the box is made of transparent PMMA with thickness 3 mm. One of the sides has a transparent bottom slit of height h, matching the solution thickness. This side slit faces a blue LED with wavelength 470 nm (CCS, LFV3-G-50X100BL), and intensity $I \in [0.05; 0.5]\,\mathrm{W/m^2}$ measured at the box wall with a light-meter (Thorlabs, S170C). A red collimated LED (Advanced illumination, CX0404-625IC) below the box shines light through the algal culture with typical intensity $0.8\,\mathrm{W/m^2}$. We observe from the top with a camera (Nikon, $\mathrm{D800_E}$) mounted with a macro 105 mm objective (Sigma), taking images every 30 s. The whole setup lays inside a larger black enclosure to prevent parasite light.

Note that the combination of flat-walled container and linear side blue LED ensures a uniform illumination at the exposed wall. As demonstrated by experimental observations in Figure 2, this guarantees a quasi-homogeneous environment in the spanwise direction (y-axis) along the wall.

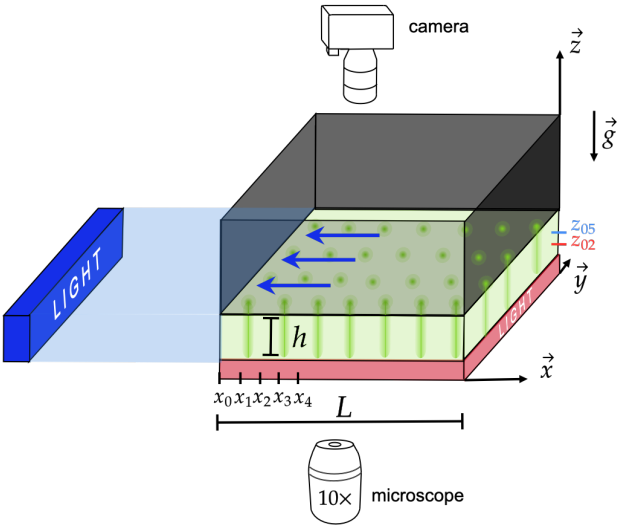


Figure 1. Experimental setups. A box with opaque black side walls contains algae (green area). Darker green dots stand for plumes. A blue side light on the left induces phototactic migration, stressed by the blue arrows. Macro experiments: red backlightning enables plumes observation from the top with a camera. Micro experiments: algal dynamics is recorded from below with a 10× objective, under an inverted microscope, shining red light. The x-axis is aligned with the blue light beams, pointing away from the lamp. The y-axis is orthogonal to the light beam and the z-axis points upwards in a direct system. The origin is taken at the bottom left box corner, close to the light. Intermediate depths labelled z_{02} and z_{05} respectively correspond to $0.2h$ and $0.5h$. The x_i positions highlight measurement spots away from the wall.

Microscopic experimental setup. We build a miniaturised version to observe the dynamics under an inverted microscope (Leica, DMI8). A red filter (Edmund Optics, RG630) through the illumination path offers red illumination. The smaller box now has a shorter side length $L = 4.3\,\text{cm}$ and a width 7.5 cm, glued over a 1 mm-thick-glass slide to maximise light transmission. As CR cultures strongly absorb light, we lower the bath thickness and fix $h = 1\,\text{mm}$ to observe individual algae at various depths. An optical fiber (Thorlabs, M470L5) provides the side blue light (470 nm) with intensity $I \in [0.05; 0.5]\,\text{W/m}^2$. The microscope itself is protected by a black enclosure to prevent parasite light interfering with our experiments.

These two experimental setups offer to analyse the phenomenon at different levels. With the macroscopic setup, we measure the local cell concentration through grey levels, at a millimetric scale in the (x, y)-plane. We observe this concentration averaged over the thickness of the liquid (z-axis). Conversely, in the microscopic configuration, we track single cells at selected z-planes. This offers access to the local cell dynamics for various depths.

2.2. *Algal culturing*

We grow synchronised cultures of two strains of *Chlamydomonas reinardtii*: wild type CC125 and short flagella mutant CC3663 shf1 mt+ from the Chlamydomonas Center, Minnesota. Results are

qualitatively similar with both strains. Here we present results obtained with the latter. We grow them in Tris-Acetate-Phosphate (TAP) medium at 22 °C under a diurnal cycle of 14:10 hours of light (6.4 W/m^2) and darkness in a programmable incubator (Memmert, IPP260ECOPLUS) [30]. We use 50 mL of TAP in 250 mL Erlenmeyers, under constant agitation at 120 rpm (Heidolph Rotamax 120 orbital shaker). We sample algae at the end of their exponential growth, about 7 days after inoculation. Long term storage is made on agar slants, by adding 1.5% of agar in our TAP solution. To check now and then the absence of bacterial contamination, we sometimes add 0.4% of yeast extract to the solid preparation. Every month, we make a new slant and start new liquid cultures.

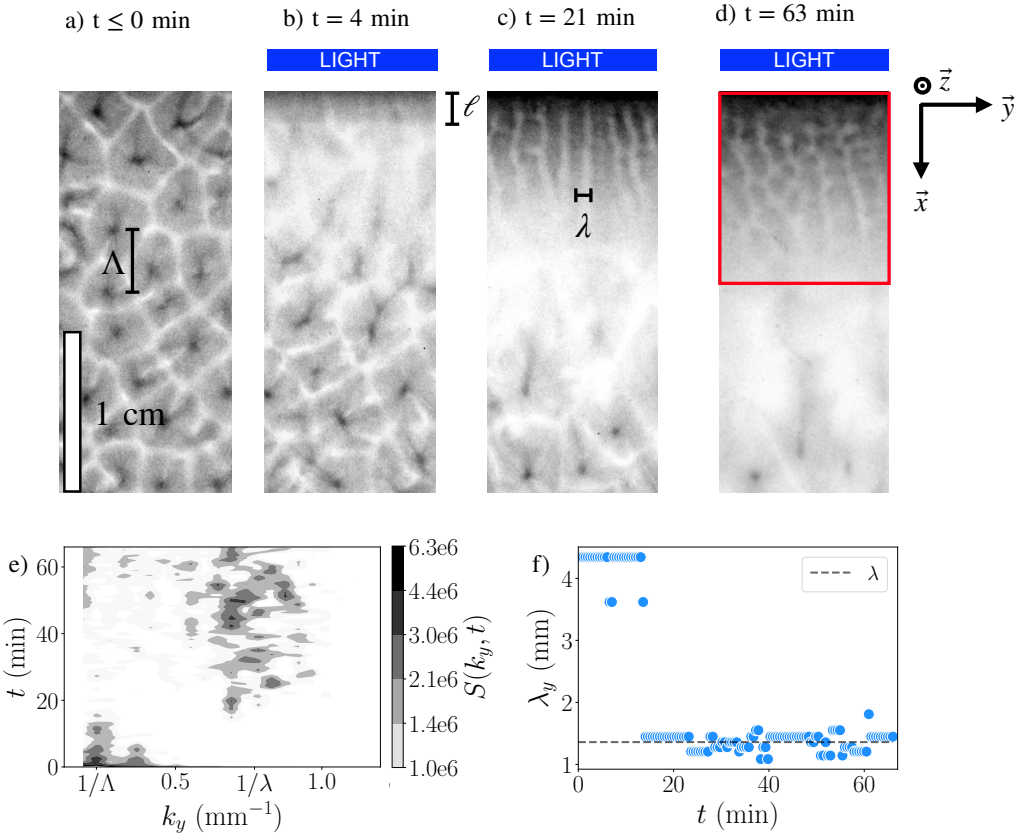


Figure 2. Experimental observations, top views: CR culture with concentration $c = (7 \pm 1) \cdot 10^6$ cells/mL, bath thickness $h = 4$ mm. (a) Initial culture in the dark, showing plumes of bioconvection spaced by Λ. (b) 4 minutes after light is switched on, with intensity $I = (0.2 \pm 0.03)$ W/m^2 from the top of the picture. Plumes are cleared away and the grey zone extends over ℓ. (c) At $t = 20$ min, a periodic structure with wavelength λ appears, perpendicular to the illuminated wall. (d) At $t = 63$ min, the pattern breaks up into smaller patches, advected away from the light towards the center of the box. (e) Spectrogram of $S(k_y, t)$ showing the average spectrum of the 1D FFT performed on each line within the red rectangle. (f) Time evolution of the dominant wavelength λ extracted from the spectrogram.

2.3. *Experimental protocol*

We leave algae in complete darkness for 30 min before each experiment. This acclimatisation ensures that prior light exposure does not influence the phototactic behaviour [31]. Plumes of

bioconvection spontaneously form in the dark (see Figure 2(a)) [3]. Once they appear, we switch on the side blue light (Figure 2(b)–(d)). For experiments under the microscope, the thickness is too shallow ($h \leq 1\,\text{mm}$) to observe the onset of bioconvective plumes. Thereby, we start the experiment once acclimatisation is over and we observe algal dynamics close to the enlightened wall. We validate that both experiments track the same phenomenon by observing the rise of the anisotropic pattern at the illuminated wall (see the supplementary material [32]). We start measurement after 30 min of illumination.

2.4. *Image analysis*

Macroscopic experimental setup. To follow the temporal and spatial evolution of the pattern, we use our top-view images. We focus the analysis close to the illuminated wall where the anisotropic structures develop, highlighted by the red rectangle in Figure 2(d). At each time τ, we conduct a 1D Fourier analysis for each line parallel to the wall (given x^*, variable y), obtaining the spectra $A(k_y)^{x^*,\tau}$. We then average over all $x^* \in [0;\, \ell]$ those spectra to get a single spectrum $A(k_y)^t = \left\langle A(k_y)^{x^*,\tau} \right\rangle_x$ and the associated power spectrum $S(k_y)^\tau = \left|A(k_y)^\tau\right|^2$. We stack each power spectrum to build the spectrogram of $S(k_y, t)$ in Figure 2(e). Two characteristic wavelengths emerge, corresponding to plumes of bioconvection (Λ) and to the elongated structures at the wall (λ). We follow their extent and dynamics on the spectrogram (Figure 2(e)). Additionally, we plot in Figure 2(f) the temporal evolution of the dominant wavelength $\lambda(t) = 1/k_{y,m}(t)$, with $k_{y,m}(t)$ the wavenumber maximising $S(k_y, t)$ at each time step. Python scripts related to this analysis are available in the supplementary material.

Microscopic experimental setup. We track individual algae in a horizontal plane (fixed depth z) under the microscope. For this purpose, we analyse our videos with the TrackMate plugin in *ImageJ*, keeping trajectories longer than 30 µm to avoid dead- and ill-cell detection. Then, we compute the average velocity u of each swimmer in the x-direction, that is, the direction aligned with the light source. The mean velocity of the entire population is $U = \overline{u}$ and its uncertainty is taken as the standard deviation of u. Python scripts related to this analysis are also available in the supplementary material.

3. Results

An initially homogeneous CR culture with concentration $c = (7 \pm 1) \cdot 10^6$ cells/mL and thickness $h = 4\,\text{mm}$ spontaneously destabilises after a few minutes in the dark (see supplementary movie). Grey shades in Figure 2(a)–(d) highlight the uneven concentration field, averaged over the thickness of the bath. Downwelling plumes, highly concentrated in microswimmers, are associated with the darker spots [2]. Their wavelength is $\Lambda = (4.2 \pm 0.2)\,\text{mm}$, close to the liquid depth h. At $t = 0$ (Figure 2(a)), we switch on the blue side light. Within a minute, plumes vanish close to the illuminated wall. Away from the light, bioconvective cells remain unaffected. A couple of minutes later, plumes vanish over a larger extent into the box and a darker band of size $\ell \approx 2\,\text{mm}$ appears along the enlightened wall (Figure 2(b)), stressing that algae accumulate at the wall, in positive phototaxis. During the next half hour, plumes disappear further away and the grey band continues to extend into the container, up to $\ell \approx 8\,\text{mm}$, at a typical speed of 5 µm/s (see time sequence Figure 2). Surprisingly, around $t \approx 8\,\text{min}$, the grey band evolves and a new pattern arises. As visible in Figure 2(c), elongated structures appear, perpendicular to the illuminated wall. These structures align with the direction of the light. The new pattern starts about 4 mm away from the wall and extends into the container over the rest of the grey band. The x-aligned, elongated pattern is regularly spaced in the y-direction and a characteristic wavelength emerges, sensibly

smaller than Λ. About half an hour later, the pattern evolves again and becomes unsteady: the parallel structures now split into smaller patches (Figure 2(d)) which are advected away from the light, towards the center of the container.

A Fourier analysis of our experiments supports this description. We focus here on the zone close to the wall, highlighted by the red rectangle (see the supplementary material for the analysis over the whole image). The spectrogram Figure 2(e) first peaks around $k_y \approx 0.23\,\mathrm{mm}^{-1}$, corresponding to $\Lambda = 1/k_y \approx 4.3\,\mathrm{mm}$, that is, the wavelength of unperturbed bioconvective plumes. Then, this peak disappears and a new band characterised by a larger wavenumber rises. The peak now lies around $k_y \approx 0.7\,\mathrm{mm}^{-1}$, and is associated with the apparition of the elongated structures. Figure 2(f) summarises this trend, as we show the wavelength $\lambda = 1/k_y$ as a function of time t, taking the maximum value of k_y at each time step. At early times, we get $\lambda_y = \Lambda \approx 4.3\,\mathrm{mm}$, the plume wavelength. At $t = 12\,\mathrm{min}$, there is a sharp transition, and the wavelength now reads $(1.4 \pm 0.1)\,\mathrm{mm}$, a third of h and Λ. This second wavelength corresponds to the regular spacing between the elongated structures at the wall.

The clearing of plumes, rise of a grey band and its subsequent patterning highlight the presence of non trivial collective motion. To get deeper insight into the dynamics of these flows and their temporal evolution, we focus on CR's dynamics at the microscopic scale. It is a challenging observation, as CR cultures at concentrations around 10^6 cells/mL are opaque. Besides, our phenomenon involves swimmers of 10 µm collectively producing millimetric patterns: pertinent lengthscales range over three orders of magnitude, an additional difficulty to catch the full dynamics at small scale. We therefore build a miniaturised version of the previous setup for observation under the microscope in a shallow bath (Figure 1). We track a population of microswimmers at various locations. This offers access to algae's speeds, but not to flow fields. Indeed, as CR are active particles, the use of the Stokes number to determine whether particles are tightly coupled to fluid flows is inappropriate [33]. Yet, as algae can be carried by faster flows which they generate [28], a precise measurement of their velocity provides valuable information.

From algae's individual trajectories, we extract the components u and v of their swimming velocities in the x- and y-directions respectively. We first present in Figure 3(a) the probability density function (PDF) of u (lines) and v (dashed lines), at two depths $z_{02} = 0.2h$ (red) and $z_{05} = 0.5h$ (blue), close to the illuminated wall ($x = x_1$). Along the x-axis, aligned with the light, at $0.5h$ (blue line), velocities are all negative and peak around $-40\,\mu\mathrm{m/s}$: algae swim towards the light source, consistent with a positive phototactic behaviour. Near the bottom of the box, at $0.2h$ (red line), swimmer's velocities are now mostly positive and peak at $30\,\mu\mathrm{m/s}$, with a small contribution in the negative range. This demonstrates that most cells are flushed away by a stronger flow, while a few of them slowly manage their way to the light. Along the wall in the y-direction, PDF are different, both peaking close to zero. This underlines the absence of net flow along the y-direction: our phenomenon appears invariant along y. In the following, we will therefore focus on velocities along the x-axis.

Algae swim on average towards or away from the light depending on their depth. To get deeper understanding into this switch, we scan across z and report $U(z) = \overline{u}(z)$, the swimming speed averaged over the population at fixed z (Figure 3(b)). We perform this vertical scan at $x_1 \approx 1\,\mathrm{mm}$. As a meniscus at the wall deviates light rays from the microscope, we cannot observe algal dynamics closer to the wall than x_1. Figure 3(b) demonstrates that a mild variation of the light intensity I does not affect our results. At $z = 0\,\mathrm{mm}$, due to adherence at the bottom surface, there is no net propulsion and $U = 0\,\mu\mathrm{m/s}$. Slightly above, for $z \in [0.1h; 0.3h]$, we report in Figure 3(b) a positive velocity U, meaning that algae are moving away from the light despite their phototactic tendency, at speeds between 40 and 50 µm/s. These measurements are in agreement with the red line of the PDF Figure 3(a). Then, at $z = 0.3h$, there is a sharp transition as U decreases up to sign reversal: algae now move to the light. When z increases further, the algal velocity becomes more

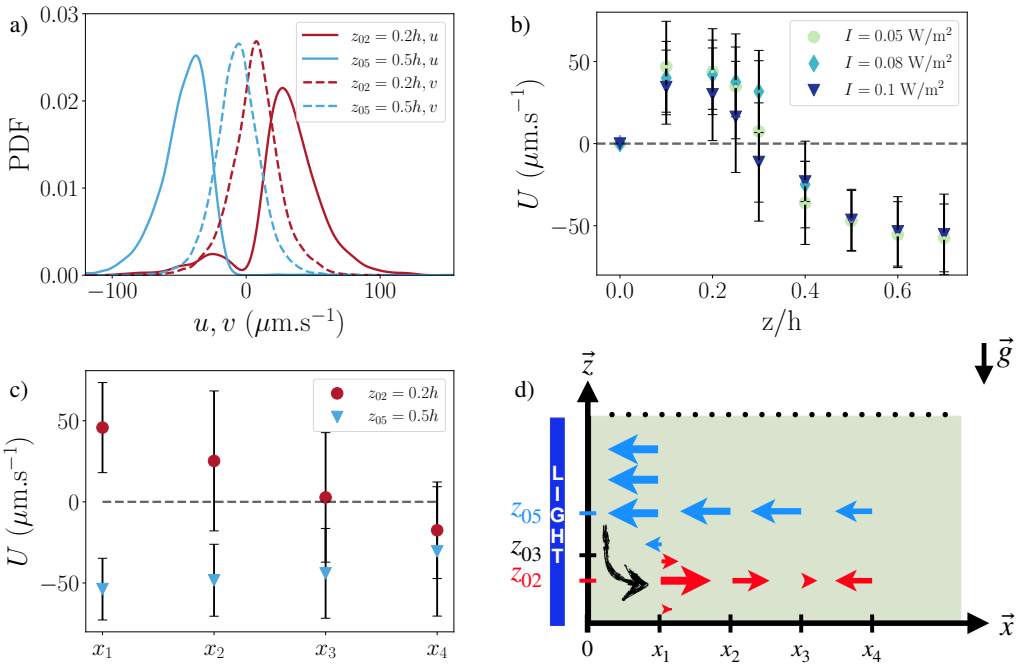


Figure 3. (a) PDF of algae's velocities u and v in the x- (solid lines) and y-direction (dashed lines) respectively, at $z_{02} = 0.2h$ (red) and $z_{05} = 0.5h$ (blue), $x = x_1$. (b) Effect of the light intensity I on the mean velocity U at various normalised depths z/h. Error bars show the standard deviation. (c) Mean velocity U away from the wall, at different x-position for z_{02} (red dots) and z_{05} (blue triangles). Data from (a)–(c) are collected with concentration $c = (7 \pm 1) \cdot 10^6$ cells/mL, thickness $h = 1$ mm and $I = (0.1 \pm 0.03)$ W/m^2. (d) Schematic of CR speeds in the (x, z)-plane, according to graphs (b) and (c). The black arrow hints CR sinking. $\vec{g}$ shows the gravity field.

negative and saturates around $-50\,\mu$m/s, close to the natural swimming speed. Due to strong light absorption by the green micro-algae, we could not acquire data further than 0.7 mm into the 1-mm-thick bath.

To get a complete picture of the dynamics near the illuminated wall, we focus on velocity variations as a function of x, at fixed depth z. In Figure 3(c), we present U at four positions, each spaced by 1 mm, starting from x_1. At mid-depth ($z = 0.5h$, blue triangles), U varies from -55 to $-30\,\mu$m/s when moving away from the light. This speed is negative, in agreement with Figure 3(a). Moreover, the intensity of the speed $|U|$ decreases, as algal swimming may be less directional when light is dissipated and absorbed far away from the wall. Closer to the bottom surface, at $z = 0.2h$ (red dots), U is first positive around $50\,\mu$m/s (see Figure 3(a)), and slowly decreases when we observe further away from the wall, until it turns negative. Then, both speeds at $z = 0.2h$ and $z = 0.5h$ converge, suggesting a homogeneous swimming speed across the whole thickness.

These experiments therefore provide an experimental evidence for two flow reversals: a first one over the thickness of the liquid (Figure 3(a) and (b)), at the illuminated wall, and a second one at the bottom of the container where algae are flushed away of the wall but swim in positive phototaxis far from the wall (Figure 3(c)). Other photo-bioconvective experiments postulated and modelled flow reversion, but its observation was hindered due to the opacity of the cultures [28]. Here, with our microscopic setup, thin enough to look through the CR population, we succeeded to experimentally observe the macroscopic photo-bioconvective flow

reversion.

4. Discussion and conclusion

We summarise our experimental observations and measurements in the schematic Figure 3(d). First, as we shine light through the culture, algae react in positive phototaxis. Individual cells swim to the light, breaking down preexisting bioconvective patterns. Knowing that water strongly absorbs light and that the phototactic reaction is proportional to the local light intensity [19,24], CR start their migration with a delay depending on their x-position away from the enlightened wall. This migration coincides with the progressive vanishing of plumes described in the time sequence of Figure 2. Then, as CR swims to the light, they accumulate at the wall where the darker band forms (Figure 2(b)). As algae further accumulate at the wall, they build up a layer denser than the surrounding medium, which eventually sinks in a classic trigger of bioconvective flows [2,27,28]. Note that, in the absence of gravity, algae would just aggregate at the illuminated wall, without sinking. Hence, the anisotropic pattern cannot be assimilated to horizontal bioconvection, provoked solely by light. Then, cells at the bottom are flushed away to the center of the box owing to mass conservation (Figure 3(b)). These cells naturally aim at reorienting to the top [12–14] and to the light [24], so that the intensity of this reverse flux slows down, until it faces the influx of phototactic cells, effectively swimming to the light (Figure 3(c)).

In summary, our experiments show the existence of a macroscopic recirculation zone in a dilute suspension of CR near an illuminated wall. In our configuration, light and swimming direction are both parallel and horizontal. The side light breaks the initial spatial symmetry as plumes vanish and CR swim to the light. Due to the wall, cells locally accumulate and surprisingly, this accumulation zone further destabilises with the emergence of an anisotropic pattern. We succeeded in observing the challenging dynamics of individual cells near the wall, enlightening the macroscopic collective motion. Further work will also focus on the hydrodynamics to explore the rise of the anisotropic pattern at the illuminated wall.

Acknowledgments

We thank Jean-François Egéa for the design and buildup of the boxes with black opaque sidewalls used in our experiments. We thank Auriane Huyghues-Despointes for intriguing side effects in her experiments, opening the door for this study. We also warmly thank José-Maria Fullana for useful discussions.

Declaration of interests

The authors do not work for, advise, own shares in, or receive funds from any organization that could benefit from this article, and have declared no affiliations other than their research organizations.

Supplementary material

The supplementary material for this article is available at https://doi.org/10.57745/OAAVBL.

References

[1] C. Dombrowski, L. Cisneros, S. Chatkaew, R. E. Goldstein and J. O. Kessler, "Self-concentration and large-scale coherence in bacterial dynamics", *Phys. Rev. Lett.* **93** (2004), article no. 098103 (4 pages).

[2] J. O. Kessler, "Co-operative and concentrative phenomena of swimming micro-organisms", *Contemp. Phys.* **26** (1985), no. 2, pp. 147–166.

[3] M. A. Bees and N. A. Hill, "Wavelengths of bioconvection patterns", *J. Exp. Biol.* **200** (1997), pp. 1515–1526.

[4] E. Shoji, H. Nishimori, A. Awazu, S. Izumi and M. Iima, "Localized bioconvection patterns and their initial state dependency in *Euglena gracilis* suspensions in an annular container", *J. Phys. Soc. Japan* **83** (2014), no. 4, article no. 043001.

[5] J. B. Loefer and R. B. Mefferd Jr., "Concerning pattern formation by free-swimming microorganisms", *Am. Natur.* **86** (1952), pp. 325–329.

[6] J. R. Platt, ""Bioconvection patterns" in cultures of free-swimming organisms", *Science* **133** (1961), pp. 1766–1767.

[7] H. W. T. Wager, "VII. On the effect of gravity upon the movements and aggregation of *Euglena viridis*, Ehrb., and other micro-organisms", *Philos. Trans. R. Soc. Lond., Ser. B* **201** (1911), pp. 333–390.

[8] O. Gallardo-Navarro, R. Arbel-Goren, E. August, G. Olmedo-Alvarez and J. Stavans, "Dynamically induced spatial segregation in multispecies bacterial bioconvection", *Nat. Commun.* **16** (2025), article no. 950 (13 pages).

[9] A. Théry, L. Le Nagard, J.-C. Ono-dit-Biot, C. Fradin, K. Dalnoki-Veress and E. Lauga, "Self-organisation and convection of confined magnetotactic bacteria", *Sci. Rep.* **10** (2020), article no. 13578 (9 pages).

[10] H. Winet and T. L. Jahn, "Geotaxis in protozoa I. A propulsion-gravity model for *tetrahymena* (Ciliata)", *J. Theor. Biol.* **46** (1974), pp. 449–465.

[11] R. Hemmersbach and R. Bräucker, "Gravity-related behaviour in ciliates and flagellates", in *Cell biology and biotechnology in space* (A. Cogoli, ed.), Advances in Space Biology and Medicine, vol. 8, Elsevier, 2002, pp. 59–75.

[12] J. O. Kessler, "Individual and collective fluid dynamics of swimming cells", *J. Fluid Mech.* **173** (1986), pp. 191–205.

[13] C. Hosoya, A. Akiyama, A. Kage, S. A. Baba and Y. Mogami, "Reverse bioconvection of *Chlamydomonas* in the hyper-density medium", *Biol. Sci. Space* **24** (2010), pp. 145–152.

[14] A. Kage, T. Omori, K. Kikuchi and T. Ishikawa, "The shape effect of flagella is more important than bottom-heaviness on passive gravitactic orientation in *Chlamydomonas reinhardtii*", *J. Exp. Biol.* **223** (2020), no. 5, article no. jeb205989 (9 pages).

[15] M. A. Bees, "Advances in bioconvection", *Ann. Rev. Fluid Mech.* **52** (2020), no. 1, pp. 449–476.

[16] S. Childress, M. Levandowsky and E. A. Spiegel, "Pattern formation in a suspension of swimming microorganisms: equations and stability theory", *J. Fluid Mech.* **69** (1975), pp. 591–613.

[17] M. Levandowsky, W. S. Childress, E. A. Spiegel and S. H. Hutner, "A mathematical model of pattern formation by swimming microorganisms", *J. Protozool.* **22** (1975), pp. 296–306.

[18] C. R. Williams and M. A. Bees, "A tale of three taxes: photo-gyro-gravitactic bioconvection", *J. Exp. Biol.* **214** (2011), pp. 2398–2408.

[19] A. A. Fragkopoulos, F. Böhme, N. Drewes and O. Bäumchen, "Metabolic activity controls the emergence of coherent flows in microbial suspensions", *Proc. Natl. Acad. Sci. USA* **122** (2025), no. 4, article no. e2413340122 (8 pages).

[20] A. Kage, C. Hosoya, S. A. Baba and Y. Mogami, "Drastic reorganization of the bioconvection pattern of *Chlamydomonas*: quantitative analysis of the pattern transition response", *J. Exp. Biol.* **216** (2013), pp. 4557–4566.

[21] N. A. Hill and T. J. Pedley, "Bioconvection", *Fluid Dyn. Res.* **37** (2005), no. 1, pp. 1–20.

[22] A. Harashima, M. Watanabe and I. Fujishiro, "Evolution of bioconvection patterns in a culture of motile flagellates", *Phys. Fluids* **31** (1988), no. 4, pp. 764–775.

[23] S. Ghorai, R. Singh and N. A. Hill, "Wavelength selection in gyrotactic bioconvection", *Bull. Math. Biol.* **77** (2015), pp. 1166–1184.

[24] K. C. Leptos, M. Chioccioli, S. Furlan, A. I. Pesci and R. E. Goldstein, "Phototaxis of *Chlamydomonas* arises from a tuned adaptive photoresponse shared with multicellular Volvocine green algae", *Phys. Rev. E* **107** (2023), article no. 014404 (25 pages).

[25] A. C. H. Tsang, A. T. Lam and I. H. Riedel-Kruse, "Polygonal motion and adaptable phototaxis via flagellar beat switching in the microswimmer *Euglena gracilis*", *Nat. Phys.* **14** (2018), pp. 1216–1222.

[26] A. Javadi, J. Arrieta, I. Tuval and M. Polin, "Photo-bioconvection: towards light control of flows in active suspensions", *Philos. Trans. R. Soc. Lond., Ser. A* **378** (2020), no. 2179, article no. 20190523.

[27] J. Arrieta, M. Polin, R. Saleta-Piersanti and I. Tuval, "Light control of localized photobioconvection", *Phys. Rev. Lett.* **123** (2019), article no. 158101 (6 pages).

[28] J. Dervaux, M. C. Resta and P. Brunet, "Light-controlled flows in active fluids", *Nat. Phys.* **13** (2017), pp. 306–312.

[29] A. Ramamonjy, J. Dervaux and P. Brunet, "Nonlinear phototaxis and instabilities in suspensions of light-seeking algae", *Phys. Rev. Lett.* **128** (2022), article no. 258101 (5 pages).

[30] E. H. Harris, D. B. Stern and G. B. Witman (eds.), "*Chlamydomonas* in the Laboratory", chap. 8, in *The Chlamydomonas Sourcebook*, 2nd edition, Academic Press Inc., 2009, pp. 241–302.

[31] T. Laroussi, M. Jarrahi and G. Amselem, "Short-term memory effects in the phototactic behavior of microalgae", *Soft Matter* **20** (2024), pp. 3996–4006.

[32] A. Givaudan, F. Picella and H. de Maleprade, *Supplementary material to "Roll formation in a bio-active fluid"*, dataset, v1, 2026. Online at https://doi.org/10.57745/OAAVBL.

[33] C. T. Crowe (ed.), *Multiphase flow handbook*, CRC Press, 2005.